Article

Cell Host & Microbe

The Host Shapes the Gut Microbiota via Fecal MicroRNA

Graphical Abstract

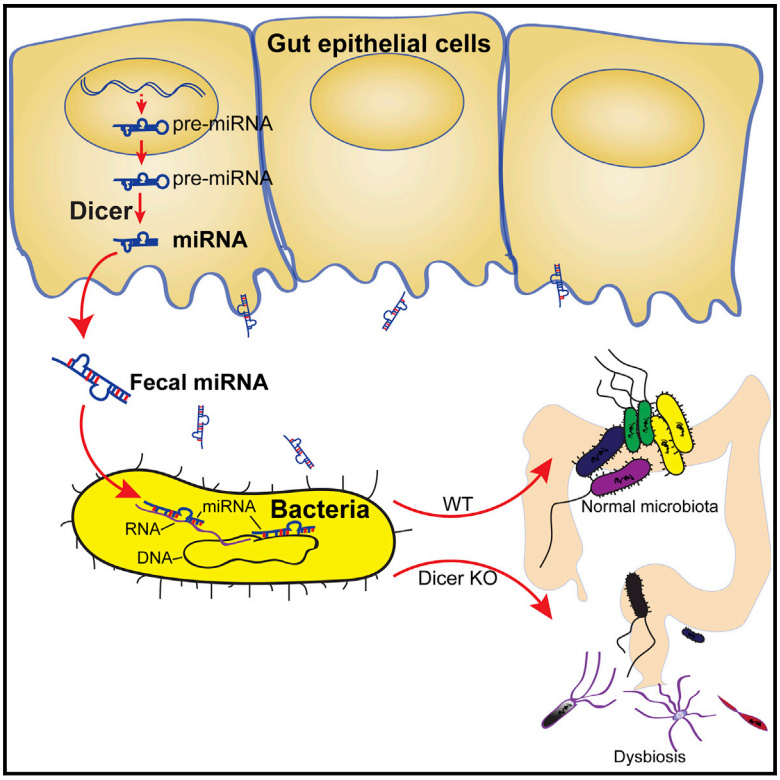

Authors

Shirong Liu, Andre Pires da Cunha, Rafael M. Rezende, ..., Laurie E. Comstock, Roopali Gandhi, Howard L. Weiner

Correspondence

hweiner@rics.bwh.harvard.edu

In Brief

How the host shapes the microbiota is unclear. Liu et al. identify host miRNAs within feces and show that these miRNAs are predominantly produced by gut epithelial cells and Hopx+ cells. These microRNAs can regulate bacterial gene expression and growth, and their loss results in imbalanced microbiota and exacerbated colitis.

Highlights

- miRNAs are normal constituents of murine and human feces
- Host gut epithelial cells and Hopx+ cells are the main sources of fecal miRNA
- miRNAs enter bacteria and regulate bacterial gene expression and growth
- Fecal miRNAs are essential for the maintenance of normal gut microbiota

Liu et al., 2016, Cell Host & Microbe *19*, 32–43
January 13, 2016
http://dx.doi.org/10.1016/j.chom.2015.12.005

CellPress

The Host Shapes the Gut Microbiota via Fecal MicroRNA

Shirong Liu,[1] Andre Pires da Cunha,[1] Rafael M. Rezende,[1] Ron Cialic,[1] Zhiyun Wei,[1] Lynn Bry,[2] Laurie E. Comstock,[3] Roopali Gandhi,[1] and Howard L. Weiner[1,*]

[1]Department of Neurology, Ann Romney Center for Neurologic Diseases, Brigham and Women's Hospital, Harvard Medical School, Boston, MA 02115, USA

[2]Department of Pathology, Brigham and Women's Hospital, Harvard Medical School, Boston, MA 02115, USA

[3]Division of Infectious Diseases, Department of Medicine, Brigham and Women's Hospital, Harvard Medical School, Boston, MA 02115, USA

*Correspondence: hweiner@rics.bwh.harvard.edu

http://dx.doi.org/10.1016/j.chom.2015.12.005

SUMMARY

The host gut microbiota varies across species and individuals but is relatively stable over time within an individual. How the host selectively shapes the microbiota is largely unclear. Here, we show that fecal microRNA (miRNA)-mediated inter-species gene regulation facilitates host control of the gut microbiota. miRNAs are abundant in mouse and human fecal samples and present within extracellular vesicles. Cell-specific loss of the miRNA-processing enzyme, Dicer, identified intestinal epithelial cells (IEC) and Hopx-positive cells as predominant fecal miRNA sources. These miRNAs can enter bacteria, such as *F. nucleatum* and *E. coli*, specifically regulate bacterial gene transcripts, and affect bacterial growth. IEC-miRNA-deficient (*Dicer1*$^{\Delta IEC}$) mice exhibit uncontrolled gut microbiota and exacerbated colitis, and WT fecal miRNA transplantation restores fecal microbes and ameliorates colitis. These findings identify both a physiologic role by which fecal miRNA shapes the gut microbiota and a potential strategy for manipulating the microbiome.

INTRODUCTION

The gut hosts a complex microbiota that is initially comprised of microbes from the mother and continues to develop through feeding and other environmental contacts (Mändar and Mikelsaar, 1996). At approximately 3 years of age in humans, the intestinal microbiota resembles an adult-like microbiota that is relatively stable over time (Faith et al., 2013; Schloissnig et al., 2013). Many factors contribute to shaping the mammalian microbiota, including host genetics, diet, and disease states (Goodrich et al., 2014; Ley et al., 2005; Turnbaugh et al., 2009). Broad trends exist within a given species, but interspecies microbial composition often differs dramatically. Reciprocal transplantation of gut microbiota into germ-free zebrafish and mouse recipients revealed that the relative abundance of microbial lineages resembles the composition of the recipient host (Rawls et al., 2006), suggesting that there are selective mechanisms in the host for the maintenance of specific components of the microbiota. Since the gut microbiota play an important role in host metabolism and immunity as well as in disease (An et al., 2014; Belkaid and Naik, 2013; Hooper et al., 2012; Iida et al., 2013; Koren et al., 2011; Smith et al., 2013; Tremaroli and Bäckhed, 2012; Turnbaugh et al., 2009), it is important to understand the mechanisms by which the microbiota is regulated by the host and to identify ways by which to manipulate the microbiome (Goodrich et al., 2014).

MicroRNAs (miRNAs) are small non-coding RNAs, 18–23 nucleotides in length, synthesized in nucleus, that are processed and function in the cytoplasm. However, increasing evidence demonstrates that miRNAs exist extracellularly and circulate in body fluids (Weber et al., 2010). Isolated studies have measured RNA in human stool and identified miRNAs as potential markers of intestinal malignancy (Ahmed et al., 2009; Link et al., 2012). Whether functional fecal miRNA exists in the normal gut is unexplored. Here we identify gut miRNAs in intestinal contents and feces and demonstrate their role in modulating the gut microbiota composition.

RESULTS

Identification of miRNA in Mouse and Human Feces

To determine whether miRNAs could be identified in the stool, we isolated RNA from both human and mouse fecal samples using the mirVana miRNA isolation kit and compared it to splenic RNA isolates. We found that both human and mouse fecal samples contained small RNA species in a pattern similar to extracellular exosome RNA (Figure S1A), whose size pattern lacks peaks for the 18S and 28S rRNA subunits (Valadi et al., 2007) as measured by bioanalyzer. We then performed small RNA bioanalyzer on the fecal samples (Figure S1B) and found three major RNA peaks in the small RNA region: ~20 nt, ~65 nt, and ~100 nt. The majority of these small RNAs were of miRNA size. In order to establish that specific miRNAs were present in mouse fecal samples, we carried out a pilot study and found that specific miRNAs could be identified by real-time quantitative PCR (qPCR) (not shown). Based on these data, we profiled mouse fecal miRNA using the NanoString nCounter platform (Geiss et al., 2008). Of the 566 miRNAs tested in mouse feces, 283 miRNAs were detected (Table S1) with miR-1224, miR-2146, miR-2134, miR-483, miR-710, miR-2141, miR-720, miR-155, and miR-34c being the most abundant miRNAs (Figure 1A).

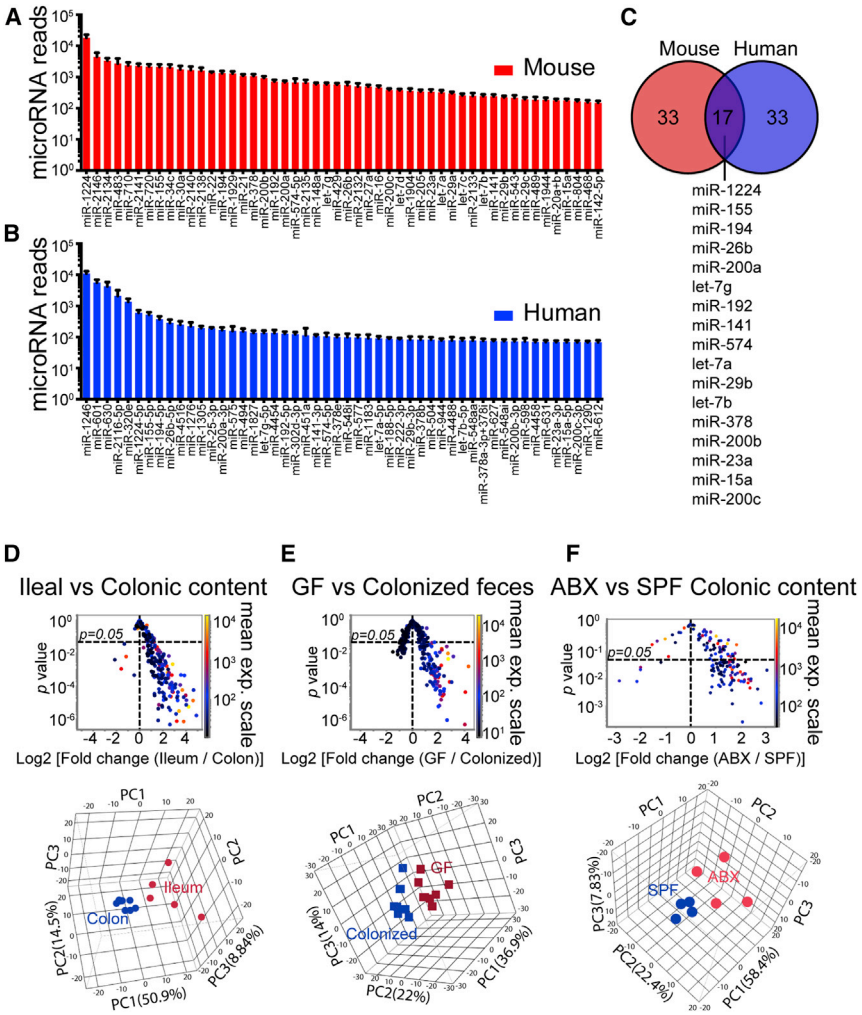

Figure 1. Identification of miRNA in Feces and Intestinal Luminal Contents

(A) Mean values ± SEM for the 50 most abundant miRNAs in mouse fecal samples (n = 6). See Table S1 for full list.

(B) Mean values ± SEM for the 50 most abundant miRNAs in human feces (n = 10). See Table S2 for full list.

(C) Venn diagram showing 17 miRNAs from the 50 most abundant fecal miRNAs shared between human and the mouse as shown in (A) and (B).

(D–F) Upper panels: volcano plots for miRNA level based on Nanostring detection in ileal luminal contents (n = 5) versus colonic luminal contents (n = 8) (D), germ-free (GF) mouse feces (n = 8) versus SPF colonized (Colonized) mouse feces (n = 8) (E), and antibiotic-treated (ABX) mouse feces (n = 4) versus SPF mouse feces (n = 4) (F). Each dot represents one miRNA; x axis: fold change; y axis: p value comparing individual miRNAs between groups (unequal variance t test followed by Benjamini-Hochberg correction); the color of the dot indicates mean expression (exp.) level of the corresponding miRNA in both groups as shown in side color scale bar. Lower panel: PCA analyses of miRNAs based on the same Nanostring datasets. See also Figure S1.

The stability of miRNAs is robust compared to mRNA (Jung et al., 2010). Extracellular miRNAs can be released in both extracellular vesicle (EV) form (e.g., microvesicle, exosome) and an EV-free form associating with high-density lipoproteins or argonaute protein. These forms may contribute to extracellular miRNA stability (Creemers et al., 2012). It was reported that epithelial cells could release exosome-like vesicles displaying major histocompatibility complexes (Van Niel et al., 2003). To explore whether EV exist in the feces, we examined the specimen with NanoSight and electron microscopy and observed EVs in the fecal samples (Figures S1C and S1D). Furthermore, we found that the most abundant miRNAs in feces, such as miR-1224, miR-2146, miR-2134, miR-2141, and miR-34c, were abundantly present in EVs (Figure S1E).

We then performed Nanostring analyses of human fecal samples to determine which miRNAs are expressed and how they compare to the ones in mouse. Of the 800 miRNAs tested in human feces, 181 miRNAs were detected (Table S2) with miR-1246, miR-601, miR-630, miR-2116-5p, miR-320e, miR-1224-5p, miR-155-5p, and miR-194-5p being the most abundant miRNAs (Figure 1B). When we compared the 50 most abundant miRNAs in mouse and human feces, we found that 17 miRNAs were shared between these species (Figure 1C).

In order to investigate whether the miRNAs are present in different sections of the gut lumen, we collected gut luminal contents from the distal ileum and colon of C57BL/6J mice, isolated RNA, and measured miRNA profiles. We observed that the miRNAs were significantly different between different regions of the intestine. More abundant miRNAs were found in the ileal lumen compared to the colon (Figure 1D). This distribution is opposite to that of the gut microbes, which are more abundant in the colon.

The gut microbiota shapes many aspects of gut physiology and immune system maturation (Lee and Mazmanian, 2010). To determine whether resident gut microbes affect fecal miRNA, we compared the fecal miRNA profile of germ-free (GF) mice with that of SPF colonized littermates. We found that the abundance of fecal miRNA in GF mice was higher than in SPF colonized mice and that the miRNA profiles in these two populations differed (Figure 1E). We further clarified this correlation by comparing SPF mice with antibiotic-treated mice and found that removal of microbes in the gut by antibiotics resulted in significantly more luminal miRNA (Figure 1F).

Intestinal Epithelial Cells and Hopx-Positive Cells are Two Main Sources of Fecal miRNA

The source of fecal miRNA has not been reported. Since intestinal epithelial cells (IECs) were reported to secret exosomes (Van Niel et al., 2003) and we observed miRNA containing exosome-like EVs in the feces (Figures S1C–S1E), we investigated whether fecal miRNAs originated from IECs. Villin protein is universally expressed in IECs. Villin-cre transgenic mice (Vil-cre) express

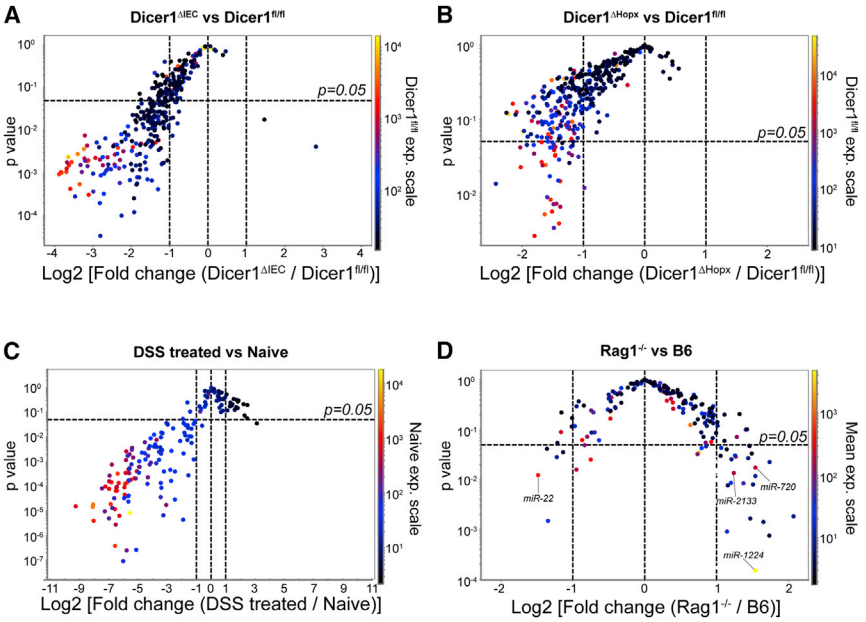

Figure 2. Intestinal Epithelial Cells and Hopx-Expressing Cells are Two Predominant Fecal miRNA Sources

Volcano plot of fecal miRNA levels detected by Nanostring in feces from: (A) Dicer1$^{\Delta IEC}$ (n = 6) versus Dicer1$^{fl/fl}$ (n = 5) mice (see also Table S3); (B) Dicer1$^{\Delta Hopx}$ (n = 4) versus Dicer1$^{fl/fl}$ (n = 4) mice (see also Table S4); (C) DSS-treated day 4 (n = 4) versus naive mice (n = 4); and (D) Rag1$^{-/-}$ (n = 5) versus wild-type C57Bl/6J (B6) (n = 5) mice. x axis: Log2 (fold change) of expression level between the groups as indicated; y axis: Benjamini-Hochberg corrected unequal variance t test p value of the compared groups. Dotted horizontal line: p = 0.05. The color of the dot indicates expression level of the corresponding miRNA in (A) and (B): Dicer1$^{fl/fl}$ (WT) group; (C): naive group; (D): mean of both Rag1$^{-/-}$ and B6 groups.

Cre recombinase under the direction of the *villin 1* promoter (Madison et al., 2002). Dicer is required for the processing of miRNAs. FloxP sites on either side of the *Dicer1* gene (*Dicer1$^{fl/fl}$*) result in the Cre-expressing cell-specific deletion of miRNAs (Harfe et al., 2005). We bred Vil-Cre mice with *Dicer1$^{fl/fl}$* mice to generate mice defective in IEC-specific miRNA (*Vil-Cre$^{Tg/-}$*, *Dicer1$^{fl/fl}$*; referred to as Dicer1$^{\Delta IEC}$ hereafter) (McKenna et al., 2010). We compared the fecal miRNA profiles of Dicer1$^{\Delta IEC}$ mice with miRNA profiles of their wild-type littermates (*Vil-Cre$^{-/-}$*, *Dicer1$^{fl/fl}$*; referred to as Dicer1$^{fl/fl}$ or WT hereafter) and found that the miRNA abundance was decreased and the profiles were altered (Figure 2A and Table S3), suggesting that intestinal epithelial cells are a major source of fecal miRNA.

We then asked whether Paneth cells and goblet cells also contributed to fecal miRNA. The HOP homeobox gene (*Hopx*) is expressed in intestinal epithelial +4 niche stem cells and in their derived cells including Paneth and goblet cells (Takeda et al., 2011). We thus bred *Hopx^{ERCre}* mice (Takeda et al., 2011) with *Dicer1$^{fl/fl}$* mice to generate *Dicer1$^{\Delta Hopx}$* (*Hopx-ERCre$^{Tg/-}$*, *Dicer1$^{fl/fl}$*; referred to as Dicer1$^{\Delta Hopx}$ hereafter) mice in which Hopx-expressing cells are deficient in miRNA following tamoxifen induction. We found that most of the detectable fecal miRNAs in Dicer1$^{\Delta Hopx}$ mice were decreased as compared to WT littermates and the profiles were changed (Figure 2B and Table S4), suggesting that the Hopx-expressing cells are also a source of fecal miRNAs. The decreased fecal miRNAs in Dicer1$^{\Delta Hopx}$ mice were different from those affected in Dicer1$^{\Delta IEC}$ mice (Tables S3 and S4), suggesting that epithelial cells and Hopx-expressing cells are responsible for the generation of different miRNAs in the feces.

To further investigate the gut epithelium as a source of fecal miRNAs, we studied dextran sulfate sodium (DSS)-induced colitis in which DSS treatment results in epithelial cell destruction and mild goblet cell loss (Solomon et al., 2010). Destruction of intestinal epithelial cells secondary to DSS treatment caused a marked decrease in fecal miRNAs (Figure 2C), supporting a key role of gut epithelial cells in the generation of fecal miRNAs. In order to distinguish whether the identified miRNAs are secreted from epithelial cells or derived from sloughed epithelial cells, we compared the miRNA profile of epithelial cells and luminal content. Although, as expected, many miRNAs were found in both luminal content and epithelial cells, we also found many miRNAs, such as miR-1224, miR-155, miR-710, and miR-2138, at a much higher abundance in the gut luminal contents compared to epithelial cells (Figure S1F), suggesting that these miRNAs are specifically secreted into the gut lumen.

To investigate the degree to which fecal miRNAs are derived from lymphocytes that may be present in the gut, we analyzed fecal miRNA in *Rag1* gene knockout mice (referred to as Rag1$^{-/-}$ hereafter), which have no mature B cells or T cells (Mombaerts et al., 1992). We found no major differences in the abundance of fecal miRNAs as compared to WT mice (Figure 2D), suggesting that these cells are not a major source of fecal miRNA.

Increased Gut Microbiota Dissimilarity in IEC miRNA-Deficient Mice

To evaluate whether fecal miRNA affects the gut microbiota, we surveyed the fecal bacterial composition of Dicer1$^{\Delta IEC}$ and Dicer1$^{fl/fl}$ littermate mice by sequencing the V4 region of 16S rRNA gene using an Illumina MiSeq platform and analyzing with the QIIME software following an established protocol (Caporaso et al., 2010). We generated over 250,000 sequences for each sample, and unique sequences were classified and grouped into 1,895 operational taxonomic units based on 97% nucleotide sequence identity (97% ID OTUs). Taxonomic classification revealed a shift of the dominant bacterial phyla Firmicutes and Proteobacteria in Dicer1$^{\Delta IEC}$ mice compared to Dicer1$^{fl/fl}$ mice (Figure S2A). At the family level, we found an increase of Bacteroidaceae and Helicobacteraceae and a decrease of Prevotellaceae, Porphyromonadaceae, Lachnospiraceae, and Ruminococcaceae in Dicer1$^{\Delta IEC}$ mice (Figure 3A). Furthermore, UniFrac metric β-diversity-based principal coordinate analysis (PCoA) showed a phylogenetic architecture that was more dissimilar within Dicer1$^{\Delta IEC}$ mice compared to

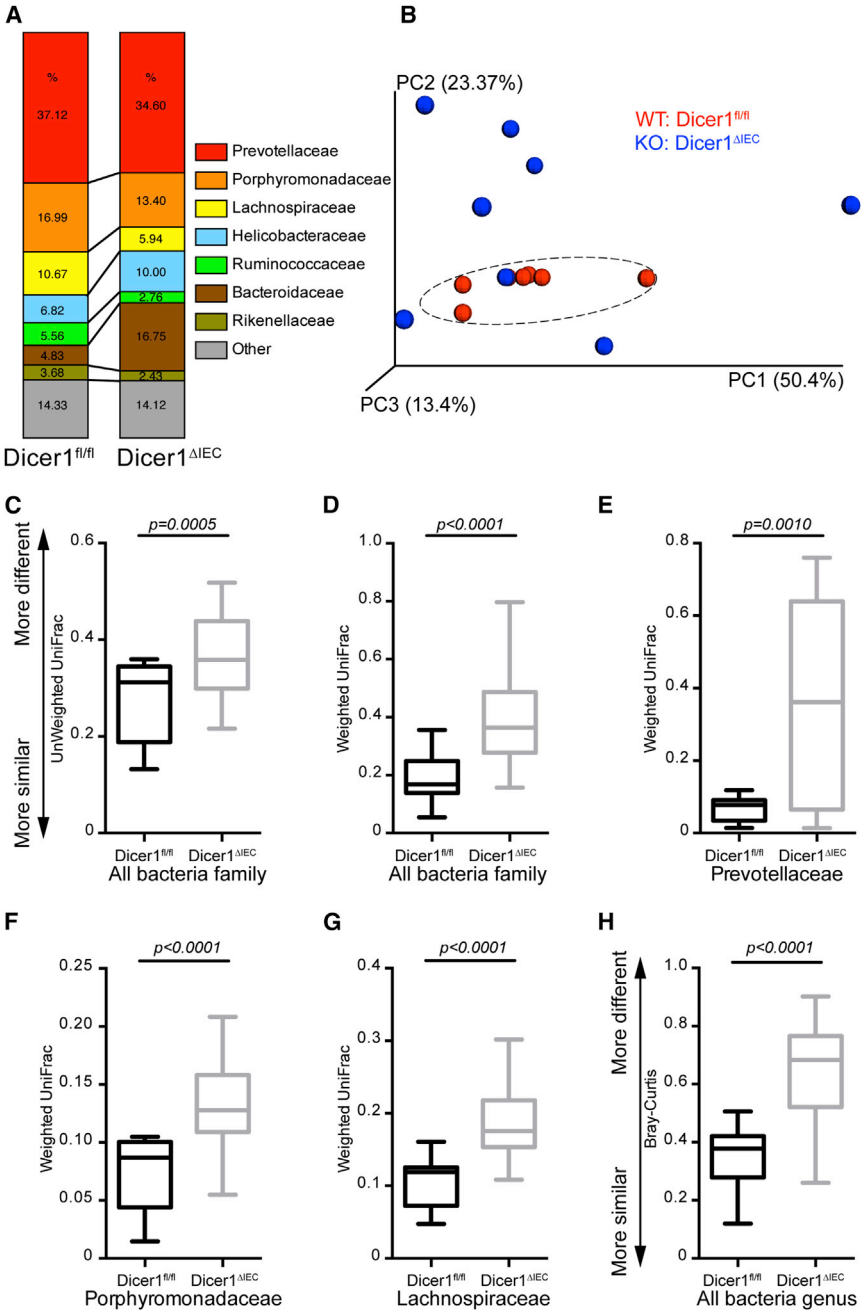

Figure 3. Deficiency of Intestinal Epithelial Cell miRNA Increases the Dissimilarity of the Gut Microbiota

Bacterial 16S rDNA sequence-based surveys were performed on the feces of 16 mice (n = 7 Dicer1$^{fl/fl}$, 9 Dicer1$^{\Delta IEC}$ mice).

(A) Relative abundance of bacteria was classified at a family-level taxonomy.

(B) Principal coordinates analysis (PCoA) based on weighted UniFrac metrics. Dashed circle indicates the clustering of Dicer1$^{fl/fl}$ samples.

(C–H) Box and whiskers plots of β-diversity distances between microbial communities comparing individuals within Dicer1$^{fl/fl}$ mice and between Dicer1$^{\Delta IEC}$ individual mice. (C–G) β-diversity at family level: (C) unweighted and (D) weighted UniFrac of the whole microbiota; (E) the bacterial family Prevotellaceae; (F) the bacterial family Porphyromonadaceae; and (G) the bacterial family Lachnospiraceae. (H) β-diversity at the genus level. (C–H) the specific distance metric used in each analysis is indicated on the axes. Values are: box, median; whiskers, min to max; p value, non-parametric t test).

See also Figure S2 and Table S5. Related to Figure 6.

WT littermates (Figure 3B), as indicated by both unweighted UniFrac analysis (Figure 3C), which measures the phylogenetic similarity between microbial communities, and weighted UniFrac analysis (Figure 3D), which is an abundance-based metric (Goodrich et al., 2014).

We then constrained the distance metric analyses to the three most dominant bacteria families detected in WT mice: Prevotellaceae, Porphyromonadaceae, and Lachnospiraceae (Figure 3A). We found marked dissimilarity between Dicer1$^{\Delta IEC}$ individuals compared to WT individuals using the weighted UniFrac metric within the Prevotellaceae family, Porphyromonadaceae, and Lachnospiraceae family (Figures 3E–3G). Within the Porphyromonadaceae and Lachnospiraceae family, we observed greater dissimilarity between Dicer1$^{\Delta IEC}$ individuals compared to WT individuals using unweighted UniFrac. However, no significant β-diversity differences were observed within Prevotellaceae families using unweighted UniFrac (Figures S2B–S2D). This indicates that the increased β-diversity within the Dicer1$^{\Delta IEC}$ mice was either from changed bacterial species or the changed abundance of particular bacteria. Furthermore, we confirmed the marked dissimilarity within Dicer1$^{\Delta IEC}$ individuals at the genus level by analyzing the overall OTU counts using Bray-Curtis β-diversity analyses (Figure 3H). Due to high β-diversity in the Dicer1$^{\Delta IEC}$ mice, we were not able to identify major individual OTU differences between Dicer1$^{\Delta IEC}$ mice and WT littermates. However, we did find 10 OTUs that had lower abundance and 2 OTUs with higher abundance in Dicer1$^{\Delta IEC}$ mice compared to WT mice (Figure S2E and Table S5).

Host miRNA Affects the Growth of Gut Bacteria

We next asked whether host miRNA affects individual microbial species in the gut. To determine whether specific miRNAs can affect bacteria directly in vitro, we examined two gut bacteria: the anaerobic species *Fusobacterium nucleatum* (*Fn*) and the facultative anaerobic species *Escherichia coli* (*E. coli*). Prior to in vitro culturing, we asked whether bacteria had any nucleic acid sites that could be targeted by miRNAs based on sequence

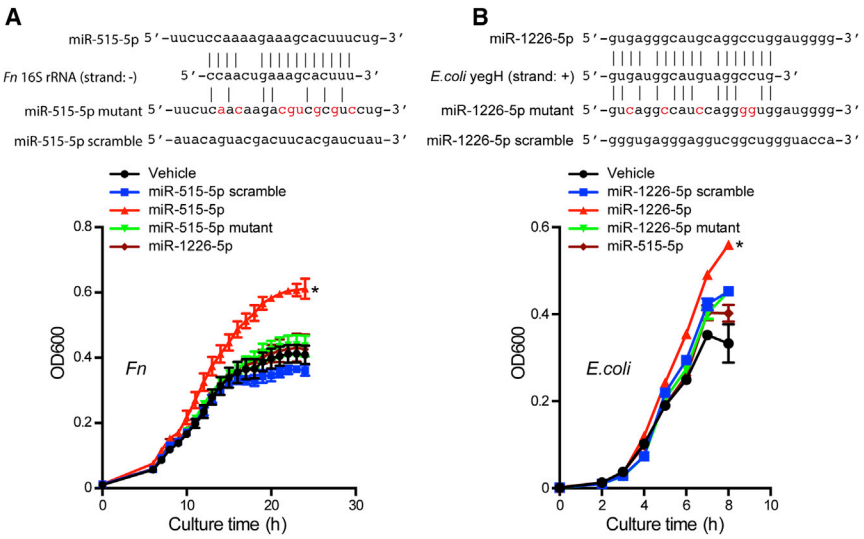

Figure 4. Host miRNA Directly Affects the Growth of Gut Bacteria

(A and B) Based on pilot culture experiments (see Figures S3C and S3F), (A) *Fn* was grown in media with 1.25 μM miRNA mimics hsa-miR-515-5p, mutated hsa-miR-515-5p, scrambled control, and hsa-miR-1226-5p. Growth was monitored as absorbance at 600 nm (OD_{600}) once per hour for 24 hr. Representative growth curves of 5 independent experiments with triplicates are presented. See Figure S3D for additional growth curves. (B) *E. coli* was grown in media with 2 μM miRNA mimics hsa-miR-1226-5p, mutated hsa-miR-1226-5p, scrambled control, and hsa-miR-515-5p. Growth was monitored as absorbance at 600 nm (OD_{600}) once per hour for 8 hr. Representative growth curves of 5 independent experiments with duplicates are presented. See Figure S3G for additional growth curves. Upper panels show target site sequence alignment of hsa-miR-515-5p and mutant (mutant site highlighted) versus *Fn* 16S rRNA (A) and hsa-miR-1226-5p and mutant versus *E. coli* yegH sequence (B). Values are mean ± SEM. *Growth differs from other groups in 5 consecutive experiments. Related to Figure S3 and Table S6.

similarity. We input seven nucleic acid sequences of *Fn*, *E. coli*, and segmental filamentous bacteria (SFB), another bacteria species that is important for gut immune development (Lee and Mazmanian, 2014), to miRBase (Griffiths-Jones et al., 2008) to search for potential targets of miRNAs. We found that each bacterial nucleic acid sequence was predicted to be targeted by many miRNAs (Figure S3A and Table S6). Notably, these miRNAs come from both lower species, such as worm (*Caenorhabditis elegans*) and fly (*Drosophila melanogaster*), and higher species, including mouse and humans (Figure S3A and Table S6). The miRNA could align to either the plus or minus strand and thus potentially act at the DNA level to affect gene expression or directly on RNA. Among these miRNAs, we found that miR-101, hsa-miR-515-5p, miR-876-5p, hsa-miR-325, and hsa-miR-1253 could potentially target *Fn* nucleic acid sequences; hsa-miR-4747-3p, hsa-miR-1224-5p, hsa-miR-1226-5p, and hsa-miR-623 could potentially target *E. coli* nucleic acid sequences (Figures S3B–S3G). The abundance of these miRNAs in human feces was determined by qPCR and is shown in Figure S4A. Accordingly, we cultured *Fn* and *E. coli* with synthesized miRNA mimics of these miRNAs in vitro and found that hsa-miR-515-5p promoted the growth of *Fn* (Figures 4A and S3C), whereas hsa-miR-1226-5p promoted the growth of *E. coli* (Figures 4B and S3F). These results demonstrate that miRNAs directly affect bacterial growth. As a control, we used miRNAs that were synthesized by changing the predicted miRNA-target pairing sites of the miRNA. These mutated miRNAs did not confer the growth-promoting effect on target bacteria (Figures 4A–4B, S3D, and S3G), suggesting the effect is sequence specific.

Host miRNA Enters Bacteria and Regulates Bacterial Gene Transcripts

It has recently been reported that cellular miRNA can enter mitochondria and regulate mitochondrial gene expression (Zhang et al., 2014). It has also been well accepted that mitochondria originated evolutionarily from bacteria (Thrash et al., 2011), providing a theoretical basis for regulation of bacteria by miRNA. Thus, to elucidate how host miRNA affects bacteria growth, we first asked whether host miRNA was able to enter bacteria. We cultured a GFP-expressing *E. coli* strain (*E. coli*-GFP) with different synthesized fluorescence (Cy3)-conjugated miRNAs and examined the *E. coli*-GFP by confocal microscopy. We found that miRNAs entered the bacteria and co-localized with bacterial nucleic acids (Figures 5A–5D and Movie S1). Additionally, Cy3-conjugated miRNAs were also observed to co-localize with nucleic acids in *Fn* (Figures S4B–S4E and Movie S2). Furthermore, we observed the dynamic accumulation of miRNA in bacteria by flow cytometry during culture (Figures 5E and 5F), providing a temporal and spatial basis for miRNA-bacterial nucleic acid interaction. Notably, the different capability of different miRNAs to enter bacteria may in part explain different miRNA effects on bacteria gene transcripts and growth.

To further examine the effect of the interaction of host miRNA with bacteria, we asked whether the bacterial gene expression could be specifically affected by the introduced miRNA. We cultured *Fn* with human miR-515-5p and quantified the 16S rRNA transcripts by qPCR. As we predicted (Figure 4A), the ratio of *Fn* 16S rRNA/23S rRNA transcripts was increased (Figure 5G). Similarly, *E. coli* yegH mRNA was increased by miR-1226-5p (Figure 5H), RNaseP was increased by miR-4747-3p (Figure S4F), rutA mRNA was decreased by miR-1224-5p (Figure S4G), and fucO was decreased by miR-623 (Figure S4H). In order to investigate whether the regulation is sequence specific, we disrupted the predicted base pairing by using mutated miRNAs and determining gene regulation and growth effects. Because the most profound bacterial growth interference effect was miR-515-5p on *Fn* (Figure S3C) and miR-1226-5p on *E. coli* (Figure S3F), we mutated the predicted pairing sites of miR-515-5p and miR-1226-5p (Figure 4). These alterations not only impaired the gene regulation of the miRNAs (Figures 5G and 5H) but also impaired their growth-enhancing effects (Figures 4, S3D, and S3G).

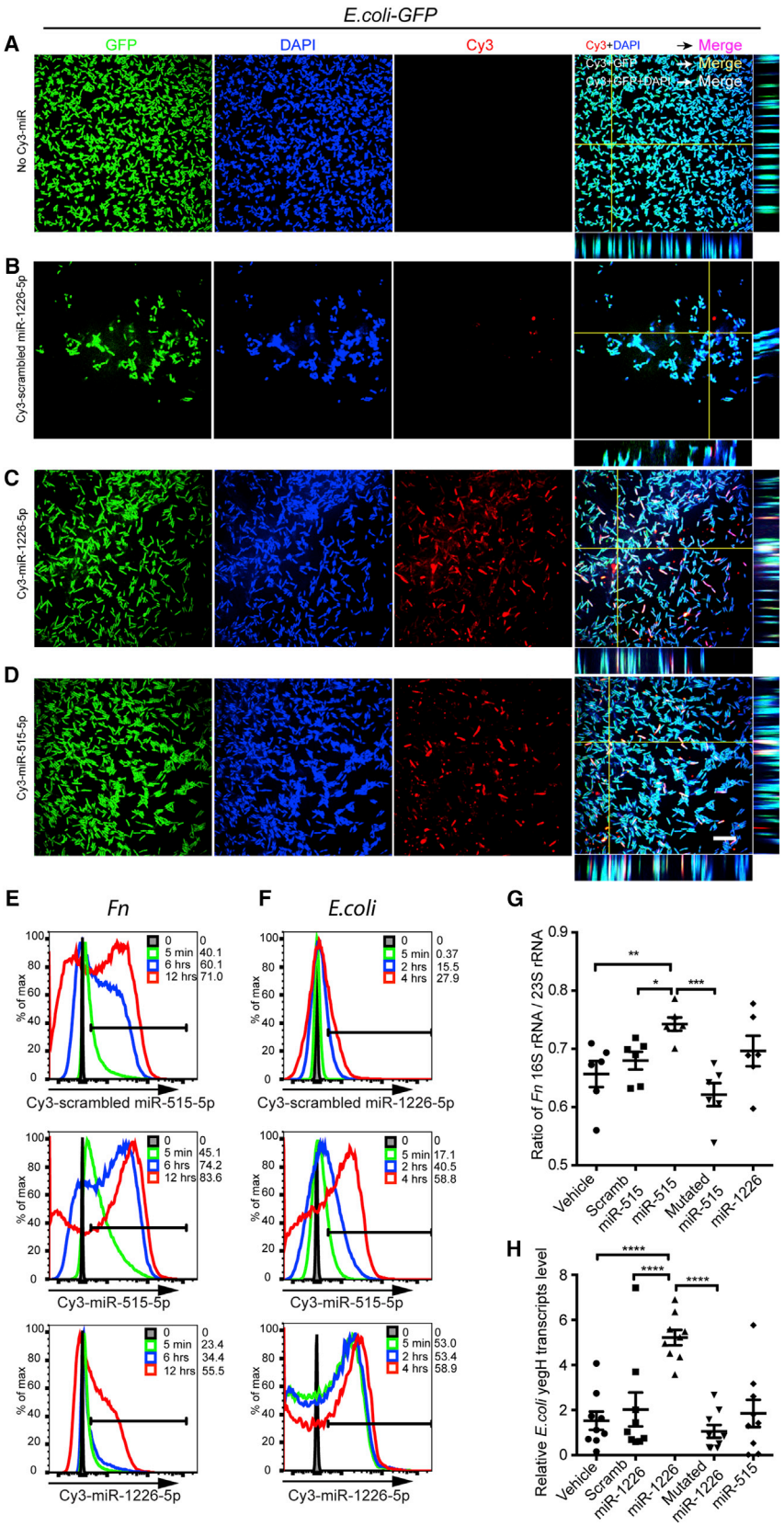

Figure 5. Host miRNA Enters Bacteria and Specifically Regulates Bacterial Gene Transcripts

(A–D) *E. coli*-GFP (green) was cultured in the presence of 2 μM Cy3-labeled (red) hsa-miR-1226-5p, scrambled hsa-miR-1226-5p control, or hsa-miR-515-5p for 4 hr and washed with PBS, and fixed in 2% PFA, followed by nucleic acid staining with DAPI (blue). Images were acquired by confocal microscopy with a 100× objective. Merged channel and orthogonal view were processed with Fiji/ImageJ. Scale bars, 10 μm. Representative of 2 experiments (see also Movie S1).

(E) *Fn* was cultured in the presence of 1.25 μM Cy3-labeled (red) hsa-miR-515-5p, scrambled hsa-miR-515-5p control, or hsa-miR-1226-5p for 0, 5 min, 6 hr, and 12 hr and terminated on ice, washed once with cold PBS, and fixed with 2% PFA, followed by flow cytometry detection of Cy3 in the bacteria. The percentage of Cy3-miR positive *Fn* is shown. Representative of 2 experiments.

(F) *E. coli*-GFP was cultured in the presence of 2 μM Cy3-labeled (red) hsa-miR-1226-5p, scrambled hsa-miR-1226-5p control, or hsa-miR-515-5p for 0, 5 min, 2 hr, and 4 hr and terminated on ice, washed once with cold PBS, and fixed with 2% PFA, followed by flow cytometry detection of Cy3 in the GFP^+ *E. coli*. The percentage of Cy3-miR positive *E. coli* is shown. Representative of 2 experiments.

(G) *Fn* was cultured in the presence of vehicle, 1.25 μM scrambled hsa-miR-515-5p control, hsa-miR-515-5p, mutated hsa-miR-515-5p, or hsa-miR-1226-5p for 16 hr. RNA was isolated, and the ratio of *Fn* 16S rRNA/23S rRNA transcript level was quantified by qPCR.

(H) *E. coli* was cultured in the presence of vehicle, 1.25 μM scrambled hsa-miR-1226-5p control, hsa-miR-1226-5p, mutated hsa-miR-1226-5p, or hsa-miR-515-5p for 4 hr. RNA was isolated, and transcript levels of *E. coli* yegH were quantified by qPCR.

(G and H) Values are mean ± SEM, one-way ANOVA followed by Dunnett's multiple comparison tests. $^*p < 0.05$, $^{**}p < 0.01$, $^{***}p < 0.001$, $^{****}p < 0.0001$. Data summarize 3 independent experiments.

See also Figure S4.

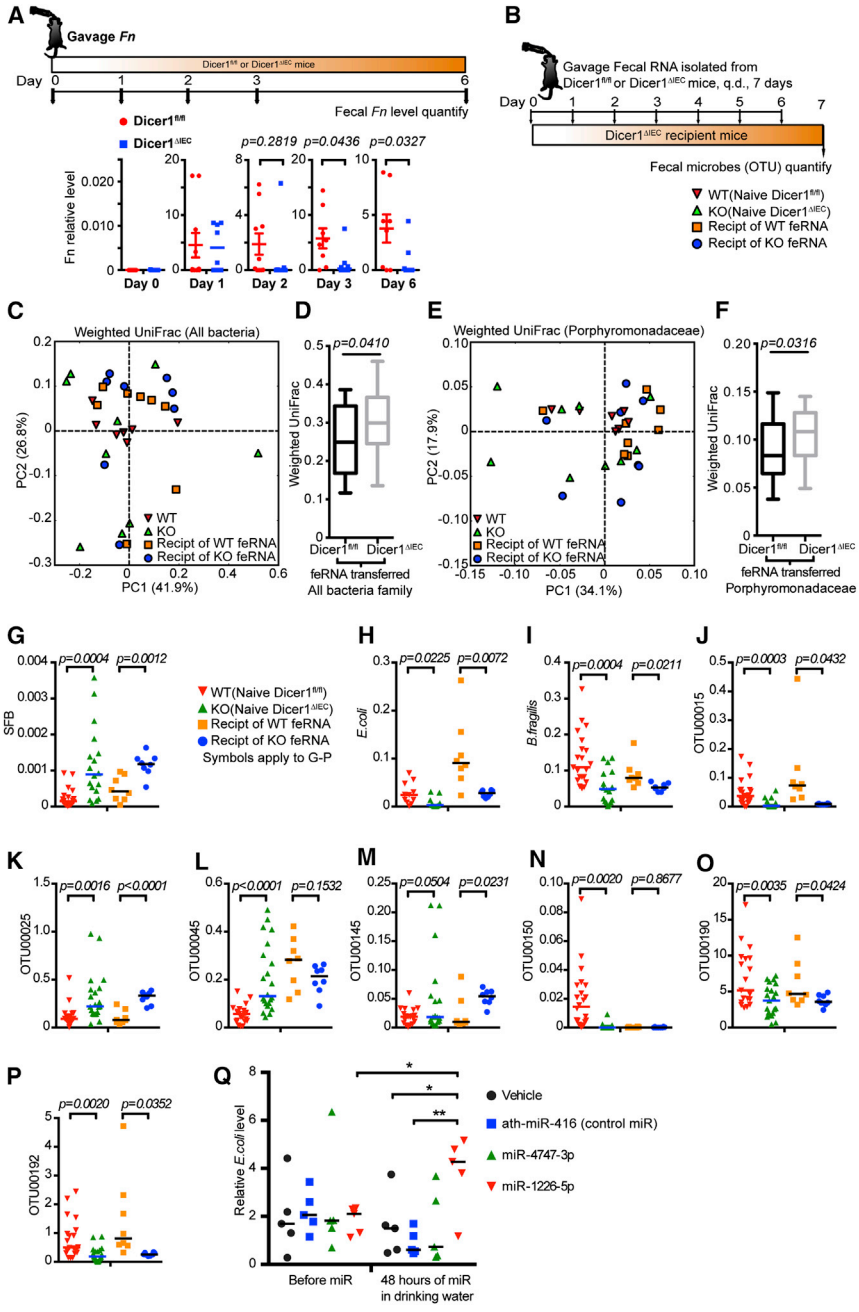

Figure 6. WT Fecal RNA Transplantation Restores the Fecal Microbes in IEC miRNA-Deficient Mice

(A) WT (Dicer1$^{fl/fl}$) or Dicer1$^{\Delta IEC}$ mice were gavaged *Fn*. The relative abundance of *Fn* in the mouse feces was monitored by qPCR at gavage (day 0), day 1, day 2, day 3, and day 6 post-gavage. Data are mean ± SEM, t test, n ≥ 8 mice and 6 littermate pairs per group, summary of two independent experiments.

(B) Schematic diagram of fecal RNA transplantation that applies to (C)–(P): donor fecal RNA (feRNA) was isolated from Dicer1$^{fl/fl}$ or Dicer1$^{\Delta IEC}$ mice and was transferred by gavage once daily (q.d.) for 7 days to Dicer1$^{\Delta IEC}$ recipient mice (Recipt), one donor to one recipient.

(C–F) Bacterial 16S rDNA sequence-based UniFrac similarity matrix of the 18 recipient mice (n = 8 Dicer1$^{fl/fl}$ fecal RNA recipients, 8 Dicer1$^{\Delta IEC}$ fecal RNA recipients) was performed on the feces and compared with naive mice as presented in Figure 3 of the Dicer1$^{fl/fl}$ and Dicer1$^{\Delta IEC}$ mice. (C and E) PCoA of weighted UniFrac values of 4 groups. Each point represents one mouse sample, and each sample is colored according to gene background or treatment. (C) Weighted UniFrac PCoA clustering results for all bacteria. (E) Weighted UniFrac PCoA clustering results for the family of Porphyromonadaceae. (D and F) Box and whiskers plots of β-diversity UniFrac values between individuals within Dicer1$^{fl/fl}$ fecal RNA recipients and between Dicer1$^{\Delta IEC}$ fecal RNA recipients of all bacteria (D) and the bacterial family Porphyromonadaceae (F). Values are: box, median; whiskers, min to max; p value, non-parametric t test.

(G–P) Symbiotic bacteria SFB (G), *E. coli* (H), *B. fragilis* (I) loads in the naive Dicer1$^{fl/fl}$ and Dicer1$^{\Delta IEC}$ mouse feces, as well as in the feces of Dicer1$^{\Delta IEC}$ mice received fecal RNA transfer were determined; and the loads of the bacterial OTU00015 (J), OTU00025 (K), OTU00045 (L), OTU00145 (M), OTU00150 (N), OTU00190 (O), and OTU00192 (P) as tagged in Figure S2E were determined by qPCR (naive group, n ≥ 11, fecal RNA transplanted group, n = 8; scatter dot plot with line at median, t test).

(Q) C57BL/6J mice were administered 200 nM indicated synthesized miRNA mimics in drinking water for 48 hr, and the relative abundance of *E. coli* in the feces was determined by qPCR (n = 5, scatter dot plot with line at median, one-way ANOVA followed by Dunnett's multiple comparison tests; *p < 0.05, **p < 0.01).

Related to Figures 3 and S5.

WT Fecal miRNA Transplantation Restores the Fecal Microbes in IEC miRNA-Deficient Mice

Our in vitro bacteria culture data suggest that miRNAs regulate bacterial genes and a bacterial gene could be targeted by multiple miRNAs. We thus hypothesized that a set of host fecal miRNAs could contribute to shaping the composition of the gut microbiota. To investigate whether miRNAs in the gut affect the growth of exogenously introduced bacteria, we gavaged Dicer1$^{\Delta IEC}$ mice and their WT littermates with *Fn*, which is not normally present in mouse feces. We found a significantly higher level of *Fn* in the feces of WT mice compared to feces from Dicer1$^{\Delta IEC}$ mice (Figure 6A).

We then asked whether the endogenous microbes in the gut would also be directly shaped by fecal miRNAs. We performed a compensation assay. In this assay, RNA was isolated from WT or Dicer1$^{\Delta IEC}$ mouse feces and then administered to Dicer1$^{\Delta IEC}$ recipient mice by gavage, one donor to one recipient (Figure 6B). 7 days after fecal miRNA transplantation, the microbiota profile of the recipient mice was examined by 16S rDNA sequencing. We found that transfer of WT fecal RNA, as

compared to transfer of Dicer1$^{\Delta IEC}$ fecal RNA, more profoundly reduced the gut microbiota β-diversity in KO recipients to be more similar to that of WT as evaluated by weighted UniFrac analyses of the whole microbiota (Figures 6C and 6D) and of the family Porphyromonadaceae (Figures 6E and 6F). The restoration effect was confirmed by a qPCR platform detecting the level of three species known to influence host immune cell function (Fritz et al., 2012; Vaishnava et al., 2011) and metabolism (Chen et al., 2014), including SFB, *E. coli*, and *B. fragilis*, as well as seven highly detected OTUs. We found that SFB and OTU00025 were more abundant in naive Dicer1$^{\Delta IEC}$ mice, whereas WT fecal RNA transfer reduced their abundance (Figures 6G and 6K). *E. coli*, *B. fragilis*, OTU00015, OTU00190, and OTU00192 were increased in abundance in Dicer1$^{\Delta IEC}$ mice gavaged with WT fecal RNA transfer. Three of the ten detected species/OTUs were not restored by WT fecal RNA transfer (Figures 6G–6P).

To exclude the possibility that the changed microbiota in Dicer1$^{\Delta IEC}$ mice was due to direct effect of antimicrobial components, i.e., IgA and RegIII-γ (Hooper et al., 2012) in the host, we measured free IgA concentration in the feces and found no difference between WT and Dicer1$^{\Delta IEC}$ mice (Figure S5A). RegIII-γ expression in the small intestine did not changed either (Figure S5B), though it was increased in the colon (Figure S5C). As SFB colonize the small intestine of mice, these data collectively suggests that these host components do not contribute to compositional changes in fecal RNA-transferred Dicer1$^{\Delta IEC}$ mice. We also measured inflammatory cytokines and receptors in the colonic tissue of both naive mice and fecal RNA-transferred recipients. We found a decrease of IL-15 and TNFSF13 and an increase of TNF in naive Dicer1$^{\Delta IEC}$ mice (Figure S5D) but found no difference between the WT and Dicer1$^{\Delta IEC}$ fecal RNA-transferred recipients (Figure S5E), suggesting that the microbiota restoration effects were not mediated by antimicrobial or inflammatory components.

In order to further test whether specific miRNAs could change specific bacteria in vivo, we synthesized miR-4747-3p and miR-1226-5p that enhanced *E. coli* in vitro (Figure 4B) and placed them in the drinking water of WT mice for 48 hr. We found that supplying miR-1226-5p increased the *E. coli* abundance in the feces (Figure 6Q).

WT Fecal miRNA Transplantation Rescued DSS Colitis in Dicer1$^{\Delta IEC}$ Mice

Given our finding that the composition of the microbiota is affected by fecal miRNA, we asked if there was a physiologic consequence in Dicer1$^{\Delta IEC}$ mice. We found that the expression of MHCII in intestinal lymphoid tissue inducer cells (LTi) (Longman et al., 2014) was reduced in Dicer1$^{\Delta IEC}$ mice (Figure S6A), and this was associated with decreased expression of LT-β, IFN-γ and TGF-β (Figure S6B) in the ileum and decreased expression of IFN-γ and increased expression of IL-17 in the colon (Figure S6C). Resistin-like molecules are critical for the maintenance of colonic barrier integrity, and their expression is regulated by symbiotic bacteria (Banerjee and Lazar, 2001; Hogan et al., 2006). We found that resistin-like molecules Relm-α and Relm-β were decreased in the Dicer1$^{\Delta IEC}$ mice (Figures S6D and S6E). We further determined by qPCR the expression of epithelial tight junction molecules (Zo-1, Occludin-1, Claudin-1, Claudin-2, and Claudin-5) that were demonstrated to be regulated by symbiotic bacteria (Braniste et al., 2014). We found a significant reduction of Zo-1, Claudin-1, and Occludin-1 in the ileum (Figure S6F) and reduction of all of the tight junction protein transcripts except for Claudin-2 in the colon (Figure S6G). These changes in the Dicer1$^{\Delta IEC}$ mice increased susceptibility to colitis. Therefore, we induced colitis in mice using DSS. We found that Dicer1$^{\Delta IEC}$ mice, as compared to WT mice, exhibited greater body weight loss (Figure 7A) and shortening of the colon (Figure 7B) as well as higher cellular infiltration in the colon and extensive loss of colonic tissue integrity (Figure 7C). We next determined whether the pathology was caused by the loss of secreted fecal miRNAs or by intrinsic cellular malfunction due to deficiency of epithelial miRNA. We administered fecal RNA from WT or Dicer1$^{\Delta IEC}$ mice to Dicer1$^{\Delta IEC}$ recipient mice by gavage for 7 days prior to DSS treatment (Figure 7D). Transfer of WT fecal RNA to Dicer1$^{\Delta IEC}$ mice resulted in less body weight loss (Figure 7E), longer colon length (Figure 7F), and less severe colonic damage (Figure 7G). These data suggest that intestinal luminal miRNAs are important in protecting the integrity of the intestinal epithelial barrier.

DISCUSSION

The gut harbors approximately 10–100 trillion microorganisms, which include 100–200 different bacterial species and approximately 2–4 million genes (Faith et al., 2013). How the microbes are selected and whether the host specifically regulates microbial gene expression is not clear. Here, we identified fecal miRNAs and found that they directly regulate specific bacterial gene expression and affect gut microbial growth.

Fecal miRNAs have not been characterized in normal human and animal feces. We found that miRNAs are a normal component in feces in both mice and humans and identified gut epithelial cells and +4 niche-derived Hopx-expressing cells as two main sources of the fecal miRNAs. We found that fecal miRNAs are present in extracellular vesicles. However, since miRNAs are stable compared to other RNAs (Jung et al., 2010), whether fecal miRNAs could exist in EV-free forms, such as associating with high-density lipoproteins or argonaute protein (Creemers et al., 2012), or in a completely free form, needs further investigation.

Using miRBase (Kozomara and Griffiths-Jones, 2014), we identified that fecal miRNAs could base pair with specific bacterial genes (Table S6). By using *E. coli* and *Fn*, a species that has been reported to promote colorectal cancer (Rubinstein et al., 2013), as models, we observed that miRNAs were able to enter bacteria and co-localize with bacterial nucleic acids. This provides a temporal and spatial basis for miRNA-bacteria gene interaction. We observed that different miRNAs had different capacities to enter bacteria. This may in part explain their different regulatory effects. However, the mechanisms controlling the entry of miRNAs into bacteria, as well as the mechanisms by which miRNAs are processed after they enter bacteria, require future investigation. By using different miRNAs and mutants, we showed that specific bacterial gene transcripts were regulated by specific miRNAs in culture. Since the miRNA could align to either the plus or minus target strand, it could act at the DNA level to affect gene expression, or directly on RNA. The

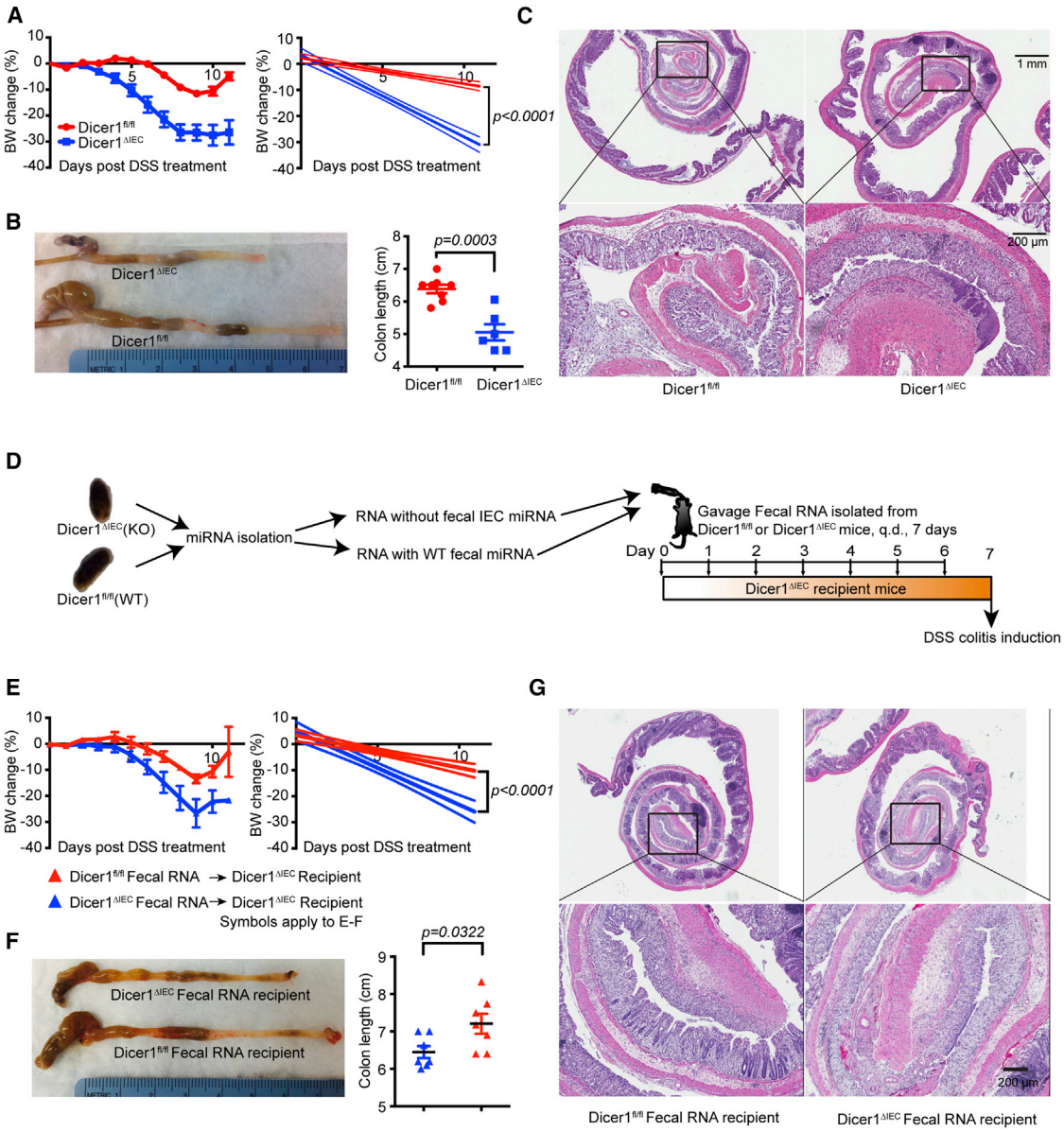

Figure 7. IEC miRNA Deficiency Is Associated with Exacerbated DSS Colitis and Is Rescued Following WT Fecal RNA Transplantation

(A–C) 6-week-old gender-matched Dicer1$^{fl/fl}$ and Dicer1$^{\Delta IEC}$ littermates were treated with 3% DSS in drinking water for 7 days. (A) Percentile change of body weight (BW). Linear regression curves of the BW change are shown in the right panel (values are mean ± SEM, $p < 0.0001$ between groups). (B) Colonic length (values are mean ± SEM, $p = 0.0003$ between groups, t test). (C) Histologic analysis (H&E) at day 9 post DSS administration (n = 8, represents two independent experiments).

(D) Schematic diagram of fecal RNA transfer and colitis induction: donor fecal RNA was isolated from Dicer1$^{fl/fl}$ (n = 8) or Dicer1$^{\Delta IEC}$ (n = 8) mice feces and was administered by gavage to Dicer1$^{\Delta IEC}$ recipient mice once daily (q.d.) for 7 days. Colitis was then induced by applying 3% DSS in drinking water for another 7 days.

(E–G) In the recipients, body weight change (values are mean ± SEM, $p < 0.0001$ between groups) (E), colonic length (values are mean ± SEM, $p = 0.0322$ between groups, t test) (F), and histologic analysis (H&E) (G) at day 9 post DSS administration were analyzed.

Related to Figure S6.

detailed mechanism by which this occurs requires further study. The bacterial regulation we describe is different from traditional miRNA regulation in eukaryotic cell posttranscriptional repression, which includes cleaving of mRNA, destabilization of mRNA, and reducing the translation efficiency (Bartel, 2009; Fabian et al., 2010). In our case, the host miRNA regulation of bacterial targets extended to rRNA (16S rRNA) and ribozyme (RNaseP), and the effect included not only a decrease of, but also enhancement of, the transcripts. However, we only observed that miR-515-5p and miR-1226-5p promoted the growth of *Fn* and *E. coli*, respectively. We did not observe a suppressive effect on growth. How miRNA regulation of gene

expression affects bacteria growth may rely on the function of the gene targeted by the miRNA.

The DSS-induced colitis model is independent of T and B lymphocytes (Dieleman et al., 1994) but dependent on symbiotic microbiota. Conventional microbiota provides a protective role in this model (Kitajima et al., 2001). By microbial 16S rRNA gene sequencing, we observed that a deficiency of epithelial-originated miRNAs resulted in a more diverse gut microbiota and changed the intestinal barrier integrity. To investigate the consequence of a changed microbiota secondary to a gut miRNA deficiency, we compared DSS-induced colitis in Dicer1$^{\Delta IEC}$ versus WT mice and found marked exacerbation of colitis in the Dicer1$^{\Delta IEC}$ mice. Importantly, we further found that fecal miRNA transplantation could help to restore the gut microbiota, which may have therapeutic applications (Goodrich et al., 2014).

In conclusion, we identified fecal miRNA as a normal component of the gut lumen. We identified host intestinal epithelial cells and +4 niche-derived cells as two main sources of fecal miRNA. We further demonstrated that fecal miRNA specifically targets bacterial genes and thus regulates the gut microbiota. Given the importance of gut microbiota in host physiology and pathology (Honda and Littman, 2012), our findings reveal a host defense mechanism and highlight miRNA as a strategy for specific manipulation of microbiome for the health of the host.

EXPERIMENTAL PROCEDURES

For detailed procedures, see the Supplemental Experimental Procedures.

Animals, Tissue, and Feces Sampling

Animals were handled according to protocols approved by the Harvard Medical Area (HMA) Standing Committee on Animals. Mouse strains B6.Cg-Tg(Vil-cre)997Gum/J (Van Niel et al., 2003) and *Hopx*$^{tm2.1(cre/ERT2)Joe}$/J (Takeda et al., 2011) were cross-bred with strain B6.Cg-Dicer1^{tm1Bdh}/J (Harfe et al., 2005). Germ-free conventionalization was performed by oral gavage SPF mouse caecal material. Fecal specimens and intestinal luminal contents were collected, snap frozen, and stored at −80°C for microbiota and miRNA analysis.

Antibiotic Treatment

Mice were given a mixture of antibiotics (ampicillin 1 mg/ml, vancomycin 500 mg/ml, neomycin 1 mg/ml, metronidazole 1 mg/ml, and streptomycin 1 mg/ml; Sigma-Aldrich) in drinking water for 1 week according to established protocols (Benjamin et al., 2013).

Human Fecal Samples

Human fecal specimens were collected from 10 healthy subjects according to a protocol approved by the Institutional Review Board at Brigham and Women's Hospital.

Fecal RNA Isolation

Total RNA (including miRNAs) was extracted from stool specimens using mirVana miRNA isolation kit (Ambion) following the manufacturer's procedure for total RNA isolation with modifications and with additional purification with Amicon Ultra-0.5 Centrifugal Filter Devices-3k (Millipore).

Quantitative NanoString nCounter Fecal miRNA Analysis

nCounter mouse miRNA Assay Kit and nCounter human miRNA Assay Kit (NanoString Technologies) were used to detect miRNA in fecal RNA isolates following the manufacturer's protocol. Assay and spike-in controls were used for normalization based on identical amounts of input RNA.

Fecal Microbes Quantification by qPCR

DNA was extracted from fecal pellets using a QIAamp Fast DNA Stool Mini Kit (QIAGEN). qPCR analysis was conducted using TaqMan Universal PCR Master Mix (Applied Biosystems).

Fecal Microbiota Diversity and Phylogenetic Analyses

16S rRNA gene V4 region amplicons from fecal DNA isolates as described were sequenced on the Illumina MiSeq 2 × 250 bp platform. Quality filtering and analysis were performed using the QIIME software pipeline following established protocols (Caporaso et al., 2010).

MiRNA Target Prediction

Nucleic acid sequences of particular bacteria were predicted for miRs targets by alignment using online miRBase tool (http://miRBase.org) (Griffiths-Jones et al., 2008).

In Vitro Bacteria Growth Measurements

Bacteria strains *Fusobacterium nucleatum* (ATCC 10953) and *E. coli* (ATCC 47016) were cultured with Mission miRNA mimics (Sigma-Aldrich) in culture medium and monitored as absorbance at 600 nm (OD_{600}).

Detection of miRNA Entering Bacteria by Confocal and Flow Cytometry

Fn and *E. coli*-GFP (ATCC 25922GFP) were cultured in the presence of synthesized Cy3-labeled hsa-miR-515-5p, hsa-miR-1226-5p, or Cy3-labeled scrambled miRNA control (GE Dharmacon) and observed with the flow cytometry and confocal microscope.

Fecal RNA Transplantation

Fecal RNA isolates from Dicer1$^{fl/fl}$ or Dicer1$^{\Delta IEC}$ mice were administered by gavage to Dicer1$^{\Delta IEC}$ recipient mice at the dosage of 22.5 μg/day for 7 consecutive days. To investigate the effect of specific miRNAs on specific bacteria, 200 nM synthesized miRNA mimics were placed in the drinking water of WT mice for 48 hr.

Bacterial Gene Transcript Quantification by qPCR

Bacterial RNA from *Fn* and *E. coli* was extracted using TRIzol MaxBacterial RNA isolation Kit (Ambion). cDNA was made, and qPCR was performed using Taqman probes. Outer-membrane protein gene gyrA and 23S rRNA were used to normalize the transcript level of *E. coli* and *Fn*, respectively.

DSS Colitis

Gender-matched 6-week-old Vil-cre$^{+/-}$-Dicer1$^{fl/fl}$ and Vil-cre$^{-/-}$-Dicer1$^{fl/fl}$ littermates were treated with 3% DSS (MW 36,000–50,000, MP Biomedicals) in the drinking water ad libitum for 7 days.

Statistical Analysis

Unless otherwise indicated, statistical significance was determined by a two-tailed Student's t test with appropriate multiple comparison correction. p value of < 0.05 was regarded as significant. Except for when specified in the context, results are expressed as mean ± SEM.

SUPPLEMENTAL INFORMATION

Supplemental Information includes Supplemental Experimental Procedures, six figures, six tables, and two movies and can be found with this article online at http://dx.doi.org/10.1016/j.chom.2015.12.005.

AUTHOR CONTRIBUTIONS

S.L. and H.L.W. conceived the concept and designed the study. S.L. generated transgenic mice and carried out all experiments. A.P.d.C. and R.M.R. were involved in cell isolation and flow cytometry. Z.W. performed extracellular vesicle isolation and NanoSight. L.B. performed GF mice colonization. L.E.C. was involved in anaerobic bacteria culture. R.G. provided human stool samples. S.L. and R.C. analyzed data. S.L. wrote the manuscript. H.L.W. supervised the study and edited the manuscript.

ACKNOWLEDGMENTS

We thank Oleg Butovsky and Duane Wesemann for providing GF and SPF colonized mice feces, technical assistance from Biopolymers Facility at Harvard Medical School for Bioanalyzer, Partners HealthCare Translational Genomics Core for sequencing, Center for Computational Cancer Biology (Dana-Farber Cancer Institute) for sequencing data analyses, DF/HCC research pathology core for histopathology, EM Facility for electron microscopy, Deneen E. Kozoriz for sorting, and Francisco J. Quintana and Vijay K. Kuchroo for helpful discussions and reading the manuscript. The research was supported by NIH grant R01 AI43458 to H.L.W. and Susan Furbacher Conroy Fellowship to S.L.

Received: June 10, 2015
Revised: November 17, 2015
Accepted: December 21, 2015
Published: January 13, 2016

REFERENCES

Ahmed, F.E., Jeffries, C.D., Vos, P.W., Flake, G., Nuovo, G.J., Sinar, D.R., Naziri, W., and Marcuard, S.P. (2009). Diagnostic microRNA markers for screening sporadic human colon cancer and active ulcerative colitis in stool and tissue. Cancer Genomics Proteomics *6*, 281–295.

An, D., Oh, S.F., Olszak, T., Neves, J.F., Avci, F.Y., Erturk-Hasdemir, D., Lu, X., Zeissig, S., Blumberg, R.S., and Kasper, D.L. (2014). Sphingolipids from a symbiotic microbe regulate homeostasis of host intestinal natural killer T cells. Cell *156*, 123–133.

Banerjee, R.R., and Lazar, M.A. (2001). Dimerization of resistin and resistin-like molecules is determined by a single cysteine. J. Biol. Chem. *276*, 25970–25973.

Bartel, D.P. (2009). MicroRNAs: target recognition and regulatory functions. Cell *136*, 215–233.

Belkaid, Y., and Naik, S. (2013). Compartmentalized and systemic control of tissue immunity by commensals. Nat. Immunol. *14*, 646–653.

Benjamin, J.L., Sumpter, R., Jr., Levine, B., and Hooper, L.V. (2013). Intestinal epithelial autophagy is essential for host defense against invasive bacteria. Cell Host Microbe *13*, 723–734.

Braniste, V., Al-Asmakh, M., Kowal, C., Anuar, F., Abbaspour, A., Tóth, M., Korecka, A., Bakocevic, N., Ng, L.G., Kundu, P., et al. (2014). The gut microbiota influences blood-brain barrier permeability in mice. Sci. Transl. Med. *6*, 263ra158.

Caporaso, J.G., Kuczynski, J., Stombaugh, J., Bittinger, K., Bushman, F.D., Costello, E.K., Fierer, N., Peña, A.G., Goodrich, J.K., Gordon, J.I., et al. (2010). QIIME allows analysis of high-throughput community sequencing data. Nat. Methods *7*, 335–336.

Chen, Z., Guo, L., Zhang, Y., Walzem, R.L., Pendergast, J.S., Printz, R.L., Morris, L.C., Matafonova, E., Stien, X., Kang, L., et al. (2014). Incorporation of therapeutically modified bacteria into gut microbiota inhibits obesity. J. Clin. Invest. *124*, 3391–3406.

Creemers, E.E., Tijsen, A.J., and Pinto, Y.M. (2012). Circulating microRNAs: novel biomarkers and extracellular communicators in cardiovascular disease? Circ. Res. *110*, 483–495.

Dieleman, L.A., Ridwan, B.U., Tennyson, G.S., Beagley, K.W., Bucy, R.P., and Elson, C.O. (1994). Dextran sulfate sodium-induced colitis occurs in severe combined immunodeficient mice. Gastroenterology *107*, 1643–1652.

Fabian, M.R., Sonenberg, N., and Filipowicz, W. (2010). Regulation of mRNA translation and stability by microRNAs. Annu. Rev. Biochem. *79*, 351–379.

Faith, J.J., Guruge, J.L., Charbonneau, M., Subramanian, S., Seedorf, H., Goodman, A.L., Clemente, J.C., Knight, R., Heath, A.C., Leibel, R.L., et al. (2013). The long-term stability of the human gut microbiota. Science *341*, 1237439–1237439.

Fritz, J.H., Rojas, O.L., Simard, N., McCarthy, D.D., Hapfelmeier, S., Rubino, S., Robertson, S.J., Larijani, M., Gosselin, J., Ivanov, I.I., et al. (2012). Acquisition of a multifunctional IgA+ plasma cell phenotype in the gut. Nature *481*, 199–203.

Geiss, G.K., Bumgarner, R.E., Birditt, B., Dahl, T., Dowidar, N., Dunaway, D.L., Fell, H.P., Ferree, S., George, R.D., Grogan, T., et al. (2008). Direct multiplexed measurement of gene expression with color-coded probe pairs. Nat. Biotechnol. *26*, 317–325.

Goodrich, J.K., Waters, J.L., Poole, A.C., Sutter, J.L., Koren, O., Blekhman, R., Beaumont, M., Van Treuren, W., Knight, R., Bell, J.T., et al. (2014). Human genetics shape the gut microbiome. Cell *159*, 789–799.

Griffiths-Jones, S., Saini, H.K., van Dongen, S., and Enright, A.J. (2008). miRBase: tools for microRNA genomics. Nucleic Acids Res. *36*, D154–D158.

Harfe, B.D., McManus, M.T., Mansfield, J.H., Hornstein, E., and Tabin, C.J. (2005). The RNaseIII enzyme Dicer is required for morphogenesis but not patterning of the vertebrate limb. Proc. Natl. Acad. Sci. USA *102*, 10898–10903.

Hogan, S.P., Seidu, L., Blanchard, C., Groschwitz, K., Mishra, A., Karow, M.L., Ahrens, R., Artis, D., Murphy, A.J., Valenzuela, D.M., et al. (2006). Resistin-like molecule beta regulates innate colonic function: barrier integrity and inflammation susceptibility. J. Allergy Clin. Immunol. *118*, 257–268.

Honda, K., and Littman, D.R. (2012). The microbiome in infectious disease and inflammation. Annu. Rev. Immunol. *30*, 759–795.

Hooper, L.V., Littman, D.R., and Macpherson, A.J. (2012). Interactions between the microbiota and the immune system. Science *336*, 1268–1273.

Iida, N., Dzutsev, A., Stewart, C.A., Smith, L., Bouladoux, N., Weingarten, R.A., Molina, D.A., Salcedo, R., Back, T., Cramer, S., et al. (2013). Commensal bacteria control cancer response to therapy by modulating the tumor microenvironment. Science *342*, 967–970.

Jung, M., Schaefer, A., Steiner, I., Kempkensteffen, C., Stephan, C., Erbersdobler, A., and Jung, K. (2010). Robust microRNA stability in degraded RNA preparations from human tissue and cell samples. Clin. Chem. *56*, 998–1006.

Kitajima, S., Morimoto, M., Sagara, E., Shimizu, C., and Ikeda, Y. (2001). Dextran sodium sulfate-induced colitis in germ-free IQI/Jic mice. Exp. Anim. *50*, 387–395.

Koren, O., Spor, A., Felin, J., Fåk, F., Stombaugh, J., Tremaroli, V., Behre, C.J., Knight, R., Fagerberg, B., Ley, R.E., and Bäckhed, F. (2011). Human oral, gut, and plaque microbiota in patients with atherosclerosis. Proc. Natl. Acad. Sci. USA *108* (*Suppl 1*), 4592–4598.

Kozomara, A., and Griffiths-Jones, S. (2014). miRBase: annotating high confidence microRNAs using deep sequencing data. Nucleic Acids Res. *42*, D68–D73.

Lee, Y.K., and Mazmanian, S.K. (2010). Has the microbiota played a critical role in the evolution of the adaptive immune system? Science *330*, 1768–1773.

Lee, Y.K., and Mazmanian, S.K. (2014). Microbial learning lessons: SFB educate the immune system. Immunity *40*, 457–459.

Ley, R.E., Bäckhed, F., Turnbaugh, P., Lozupone, C.A., Knight, R.D., and Gordon, J.I. (2005). Obesity alters gut microbial ecology. Proc. Natl. Acad. Sci. USA *102*, 11070–11075.

Link, A., Becker, V., Goel, A., Wex, T., and Malfertheiner, P. (2012). Feasibility of fecal microRNAs as novel biomarkers for pancreatic cancer. PLoS ONE *7*, e42933.

Longman, R.S., Diehl, G.E., Victorio, D.A., Huh, J.R., Galan, C., Miraldi, E.R., Swaminath, A., Bonneau, R., Scherl, E.J., and Littman, D.R. (2014). CX_3CR1^+ mononuclear phagocytes support colitis-associated innate lymphoid cell production of IL-22. J. Exp. Med. *211*, 1571–1583.

Madison, B.B., Dunbar, L., Qiao, X.T., Braunstein, K., Braunstein, E., and Gumucio, D.L. (2002). Cis elements of the villin gene control expression in restricted domains of the vertical (crypt) and horizontal (duodenum, cecum) axes of the intestine. J. Biol. Chem. *277*, 33275–33283.

Mändar, R., and Mikelsaar, M. (1996). Transmission of mother's microflora to the newborn at birth. Biol. Neonate *69*, 30–35.

McKenna, L.B., Schug, J., Vourekas, A., McKenna, J.B., Bramswig, N.C., Friedman, J.R., and Kaestner, K.H. (2010). MicroRNAs control intestinal

epithelial differentiation, architecture, and barrier function. Gastroenterology *139*, 1654–1664, 1664.e1.

Mombaerts, P., Iacomini, J., Johnson, R.S., Herrup, K., Tonegawa, S., and Papaioannou, V.E. (1992). RAG-1-deficient mice have no mature B and T lymphocytes. Cell *68*, 869–877.

Rawls, J.F.J., Mahowald, M.A.M., Ley, R.E.R., and Gordon, J.I.J. (2006). Reciprocal gut microbiota transplants from zebrafish and mice to germ-free recipients reveal host habitat selection. Cell *127*, 423–433.

Rubinstein, M.R., Wang, X., Liu, W., Hao, Y., Cai, G., and Han, Y.W. (2013). Fusobacterium nucleatum promotes colorectal carcinogenesis by modulating E-cadherin/β-catenin signaling via its FadA adhesin. Cell Host Microbe *14*, 195–206.

Schloissnig, S., Arumugam, M., Sunagawa, S., Mitreva, M., Tap, J., Zhu, A., Waller, A., Mende, D.R., Kultima, J.R., Martin, J., et al. (2013). Genomic variation landscape of the human gut microbiome. Nature *493*, 45–50.

Smith, P.M., Howitt, M.R., Panikov, N., Michaud, M., Gallini, C.A., Bohlooly-Y, M., Glickman, J.N., and Garrett, W.S. (2013). The microbial metabolites, short-chain fatty acids, regulate colonic Treg cell homeostasis. Science *341*, 569–573.

Solomon, L., Mansor, S., Mallon, P., Donnelly, E., Hoper, M., Loughrey, M., Kirk, S., and Gardiner, K. (2010). The dextran sulphate sodium (DSS) model of colitis: an overview. Comp Clin Pathol *19*, 235–239.

Takeda, N., Jain, R., LeBoeuf, M.R., Wang, Q., Lu, M.M., and Epstein, J.A. (2011). Interconversion between intestinal stem cell populations in distinct niches. Science *334*, 1420–1424.

Thrash, J.C., Boyd, A., Huggett, M.J., Grote, J., Carini, P., Yoder, R.J., Robbertse, B., Spatafora, J.W., Rappé, M.S., and Giovannoni, S.J. (2011). Phylogenomic evidence for a common ancestor of mitochondria and the SAR11 clade. Sci. Rep. *1*, 13.

Tremaroli, V., and Bäckhed, F. (2012). Functional interactions between the gut microbiota and host metabolism. Nature *489*, 242–249.

Turnbaugh, P.J., Hamady, M., Yatsunenko, T., Cantarel, B.L., Duncan, A., Ley, R.E., Sogin, M.L., Jones, W.J., Roe, B.A., Affourtit, J.P., et al. (2009). A core gut microbiome in obese and lean twins. Nature *457*, 480–484.

Vaishnava, S., Yamamoto, M., Severson, K.M., Ruhn, K.A., Yu, X., Koren, O., Ley, R., Wakeland, E.K., and Hooper, L.V. (2011). The antibacterial lectin RegIIIgamma promotes the spatial segregation of microbiota and host in the intestine. Science *334*, 255–258.

Valadi, H., Ekström, K., Bossios, A., Sjöstrand, M., Lee, J.J., and Lötvall, J.O. (2007). Exosome-mediated transfer of mRNAs and microRNAs is a novel mechanism of genetic exchange between cells. Nat. Cell Biol. *9*, 654–659.

Van Niel, G., Mallegol, J., Bevilacqua, C., Candalh, C., Brugière, S., Tomaskovic-Crook, E., Heath, J.K., Cerf-Bensussan, N., and Heyman, M. (2003). Intestinal epithelial exosomes carry MHC class II/peptides able to inform the immune system in mice. Gut *52*, 1690–1697.

Weber, J.A., Baxter, D.H., Zhang, S., Huang, D.Y., Huang, K.H., Lee, M.J., Galas, D.J., and Wang, K. (2010). The microRNA spectrum in 12 body fluids. Clin. Chem. *56*, 1733–1741.

Zhang, X., Zuo, X., Yang, B., Li, Z., Xue, Y., Zhou, Y., Huang, J., Zhao, X., Zhou, J., Yan, Y., et al. (2014). MicroRNA directly enhances mitochondrial translation during muscle differentiation. Cell *158*, 607–619.